

# No observational constraints from hypothetical collisions of hypothetical dark halo primordial black holes with Galactic objects

Marek A. Abramowicz<sup>1,2</sup>, Julia K. Becker<sup>1,3</sup>, Peter L. Biermann<sup>4,5,6,7,8</sup>  
Antonella Garzilli<sup>1,9</sup>, Fredrik Johansson<sup>1,10</sup> and Lei Qian<sup>11</sup>

## ABSTRACT

It was suggested by several authors that hypothetical primordial black holes (PBHs) may contribute to the dark matter in our Galaxy. There are strong constraints based on the Hawking evaporation that practically exclude PBHs with masses  $m_{pbh} \sim 10^{15} - 10^{16}$  g and smaller as significant contributors to the Galactic dark matter. Similarly, PBHs with masses greater than about  $10^{26}$  g are practically excluded by the gravitational lensing observation. The mass range between  $10^{16}$  g  $< m_{pbh} < 10^{26}$  g is unconstrained. In this paper, we examine possible observational signatures in the unexplored mass range, investigating hypothetical collisions of PBHs with main sequence stars, red giants, white dwarfs, and neutron stars in our Galaxy. This has previously been discussed as possibly leading to an observable photon eruption due to shock production during the encounter. We find that such collisions are either too rare to be observed (if the PBH masses are typically larger than about  $10^{20}$  g), or produce too little power to be detected (if the masses are smaller than about  $10^{20}$  g).

*Subject headings:* cosmology: dark matter — cosmology: early Universe — Galaxy: abundances — X-rays: bursts — gamma-rays: bursts

---

<sup>1</sup>Göteborgs Universitet, Institutionen för Fysik, SE-41296 Göteborg, Sweden

<sup>2</sup>N. Copernicus Astronomical Centre, Polish Academy of Sciences, Bartycka 18, 00-716 Warszawa, Poland

<sup>3</sup>Fakultät f. Physik & Astronomie, Theoretische Physik IV, Ruhr-Univeristät Bochum, Bochum, Germany

<sup>4</sup>Max Planck Institut für Radioastronomie, Auf dem Hügel 69, D-53121 Bonn, Germany

<sup>5</sup>Department of Physics and Astronomy, University of Bonn, Germany

<sup>6</sup>Department of Physics and Astronomy, University of Alabama, Tuscaloosa, AL, USA

<sup>7</sup>Department of Physics and Astronomy, University of Alabama at Huntsville, AL, USA

<sup>8</sup>Inst. Nucl. Phys. FZ, Karlsruhe Inst. of Techn. (KIT), Karlsruhe, Germany

<sup>9</sup>SISSA, via Beirut 2-4, 34151 Trieste, Italy

<sup>10</sup>Chalmers tekniska högskola, Institutionen för fundamental fysik, SE-41296 Göteborg, Sweden

<sup>11</sup>Astronomy Department, School of Physics, Peking University, Beijing 100871, P. R. China

## 1. Introduction

The idea of dark matter (DM) in the Universe was first advanced in the 1930s, when Zwicky (1933, 1937) discussed the deviation of the masses of galaxy clusters away from expected values. The idea was subsequently confirmed in many different ways (e.g. Ostriker et al. 1974; Komatsu et al. 2009). The strong deviation of the rotation curves of spiral galaxies away from what would result from just the luminous matter, has given an important additional quantitative indication of the existence of DM. Its presence in our Galaxy was first discussed by Kahn and Woltjer (1959). The current estimate gives  $M_{DM} = 9 \cdot 10^{11} M_{\odot}$  (Xue et al. 2008), which matches that by Kahn and Woltjer (1959). Searches for non-luminous DM in the form of brown and white dwarfs, neutron stars and black holes, with masses above  $0.1 - 0.2 \cdot M_{\odot}$  (“MACHOS”) has shown that these objects are far too rare to make up a significant part of the total DM (Afonso et al. 2003; Yoo et al. 2004). Within the past five years, it has even been shown by WMAP that baryonic matter only makes up  $\sim 4\%$ , of the critical density of the Universe while dark matter makes up  $\sim 20\%$  (Komatsu et al. 2009). While objects like neutron stars or white dwarfs are thereby excluded as making up a major proportion of the DM, black holes with masses between  $10^{16} \text{ g} < m_{pbh} < 10^{26} \text{ g}$  might still be responsible for a significant fraction, as explained in the next section. In certain models, these primordial black holes (PBHs) are predicted to be produced at an interesting level in early phases of the Universe due to density fluctuations of the type also observed in the cosmic microwave background. Their gravitational radius  $r_g$  would be subatomic,  $r_g \sim 10^{-8} \cdot (m_{pbh}/(10^{20} \text{ g})) \text{ cm}$ . The Bondi-Hoyle accretion radius, on the other hand, can be significantly larger.

In this paper, we check whether hypothetical PBH collisions with Galactic objects may be observable. A detection of observational signatures of such collisions would support the hypothesis that PBHs may represent a significant fraction of the DM in the Galaxy. We find that the PBH collisions discussed by Zhilyaev (2007) would produce no presently-observable signatures. To prove our case, we show that even with the most optimistic conditions assumed, hypothetical collisions of PBHs with Galactic objects place no observational constraints in the PBH mass range  $\sim 10^{16} \text{ g} < m_{pbh} < 10^{26} \text{ g}$  considered in this paper.

The assumptions made are as follows:

- The mass distribution of PBHs is a delta-function, i.e. all PBHs have the same mass. The mass is treated as a free parameter, and the whole range  $\sim 10^{16} \text{ g} < m_{pbh} < 10^{26} \text{ g}$  is considered. Any other distribution would significantly decrease the event rate: if we assume that all PBHs have the same mass and then consider this mass as a free parameter, we maximize the event rate for each single mass value, as we assume that 100% of the total mass is focused at one arbitrary value. For wider mass distributions, the total mass of the PBHs is less than 100% for a given mass value, which always reduces the event rate.
- The entire energy from a single interaction is taken to be in the energy band of the potential detector. In reality, we expect the signal to be spread from radio wavelengths up to soft

gamma-rays. Using the entire radiated energy therefore gives an upper limit for detectability.

- A single photon is sufficient for detecting the event. Even for a background-free source, three photons are required for giving 90% confidence significance (see (Amsler et al. 2008)) and so with a more realistic estimate, the detection probability would be further reduced by a factor of between 3 and more than ten.
- The signal is radiated at full opening angle, i.e.  $2\pi$ . A more realistic estimate would include consideration of the shock opening angle, reducing the expected observation probability.
- We assume that the signal is always strong enough that it can reach us over the entire thickness of the Galactic disk,  $h \approx 300$  pc.

Further, we make a few assumptions that greatly simplifies calculations but could only slightly (indeed insignificantly) influence the final result:

- Luminous matter is taken to be distributed uniformly in the Galactic disk and dark matter is taken to have constant density in the spherical halo. We will show that the enhanced density in the Galactic Center yields slightly better results, but with the same conclusion that detection of the events can be neglected.
- We use a delta-function for the distribution of relative velocity between the luminous and dark matter,  $v_0 = 2.2 \cdot 10^7$  cm/s. We will show in this paper that the reduced velocity at the central part of the Galaxy does not influence our result. As for the possibility of a capture at low velocities, we show in Section 5 that this does not occur within the energy range being considered.
- The PBH is taken to be uncharged.

For alternative approaches to explaining dark matter by extending the standard model of particle physics to include new particles, see e.g. Haber and Kane (1985); Bertone et al. (2005); Biermann and Kusenko (2006); Hooper and Profumo (2007).

In order to investigate the interaction of PBHs with objects in the Galaxy and possible observational consequences, we need to ask the following questions:

1. *How frequent are the events?*
2. *How energetic is each single event?*
3. *What are the possible signatures?*

In the following sections, we answer each question separately for the five most important object classes in the Galaxy, i.e. main sequence stars, red giants (in particular their dense cores), white

dwarfs and neutron stars. The main intrinsic properties of those objects are listed in table 1 together with their abundances in the Galaxy. Both the interaction probability and the energy loss strongly depend on the properties listed. Also, we consider collisions with the Earth, in order to investigate the claim that the Tunguska event might have been caused in this way (see Jackson and Ryan (1973)).

This paper is organized as follows. Section 2 summarizes the already-existing observational constraints. In Section 3, interaction probabilities in the Galaxy and energy loss of a single event are derived. Possible signatures and the detectability of such events are investigated in Section 4. Section 5 discusses the possibility of capturing the PBH in a stellar object. Finally, Section 6 summarizes the conclusions to be drawn from our calculations and discusses further possibilities for detection requiring additional assumptions.

## 2. Primordial black holes - constraints

Ever since the hypothesis of primordial black holes was first established (Hawking 1971), different theoretical and observational constraints on their actual abundance in the Universe have been discussed. While theoretical constraints are rather speculative and model dependent (see e.g. Carr (2005); Khlopov (2008)), the observational ones are far more robust. They firmly constrain the abundance of primordial black holes in two mass ranges. In this section, we briefly review them. Since we are interested in PBHs as a possible contributor to the dark matter, we only consider PBHs that can have survived until today, that is those with initial mass above  $5 \cdot 10^{14}$  g.

There are three main methods of looking for indirect detection of primordial black holes above  $5 \cdot 10^{14}$  g. The first one aims for the detection of PBH evaporation. This method is sensitive to the lower mass limit of the initial mass function (IMF). This initial mass function is expressed in terms of the number of PBHs at their initial mass  $m$ , as a function of the initial mass itself,  $dn/dm$ . As predicted by Hawking (1974), and shortly afterwards also by Bekenstein (1975), black holes evaporate due to quantum fluctuations around the Schwarzschild radius of the black hole, leading to the evaporation of PBHs with masses below  $5 \cdot 10^{14}$  g before the present time. Therefore, non-detection of the high-energy photons which would be produced by black hole evaporation, i.e.  $E_\gamma \gtrsim 20$  MeV, leads to a robust constraint on the mass function around  $10^{15}$  g. At  $10^{15}$  g, EGRET observations between 30 MeV and 120 MeV imply that the PBH mass density must be smaller than  $3.3 \cdot 10^{-9}$  times that of the total dark matter (Sreekumar et al. 1998; Barrau et al. 2003). Between  $10^{15} - 10^{16}$  g, constraints from EGRET measurements are still at a level of  $< 10^{-2}$  and provide significant constraints as well. At significantly higher mass scales, micro-lensing can help to restrict the abundance of PBHs, see e.g. Afonso et al. (2003). Alcock et al. (1998) looked for planetary mass dark matter via gravitational micro-lensing in the direction of the Large Magellanic Cloud, resulting in constraints of up to 10% in the mass range  $10^{26}$  g  $< m_{pbh} < 10^{33}$  g. At even higher mass scales,  $10^{33}$  g  $< m_{pbh} < 10^{40}$  g, results from anisotropy and spectra measurements of the Cosmic Microwave Background (WMAP-3years and COBE-FIRAS) can be used to constrain

the number of PBHs (Ricotti et al. 2008). The excluded regions for the mass function are shown in Fig. 1. In addition, Gould (1992) proposed using gamma ray bursts (GRBs) to detect “femto-lenses” produced by dark matter objects in the mass range of  $10^{17} \text{ g} < m_{pbh} < 10^{20} \text{ g}$ . This method has not yet been applied, however, and so no experimental limit has yet been set. A mass range of about ten orders of magnitude,  $10^{15} \text{ g} < m_{pbh} < 10^{26} \text{ g}$ , then remains at present unexplored.

In the standard scenario of density perturbations in the early Universe, the IMF of PBHs,  $dn/dm(m)$ , behaves as, e.g. Halzen et al. (1991)

$$\frac{dn}{dm} \propto m^{-2.5}, \quad (1)$$

and so most PBHs have masses at around the current evaporation level. The constraint by EGRET at the lower end of the mass scale therefore has significant consequences for the abundance of black holes at higher masses.

The above model for PBH production is not, however, the only one. Several other proposed theories for PBH production predict significant contributions from PBHs at different mass scales. Examples are the collapse of topological defects, softening of the equation of state and quantum gravity scenarios, which, although speculative, deserve to be tested (see reviews by Carr (2005); Khlopov (2008) and references therein).

### 3. A toy model to estimates of the collision probability and energetics

In order to describe possible observational signatures of the hypothetical collisions of PBHs with stars in our Galaxy, one must answer the two fundamental questions: *how frequent are the collisions?* and *how energetic is a single collision?* Precise answers to these questions are obviously very difficult to obtain, as they depend on genuine astrophysical uncertainties that cannot be resolved today. In the view of these uncertainties, we estimate the collision frequency and energetics using a very general and rather simple analytic toy model that adopts several simplifying assumptions. For example, we assume that all PBHs have the same mass  $m_{pbh}$ . We do not specify that value. Instead, we consider  $m_{pbh}$  to be one of a few free parameters of the model.

Adopting ideas from the kinetic theory of gases, one may argue that a reasonable estimate of the collision frequency between stars and PBHs should depend only on the size  $r$  of the region of interest (e.g. either the whole Galaxy, or its central bulge), numbers of stars  $N_*$  and PBHs  $N_{pbh}$  in this region, the relative velocity  $v_*$  between stars and PBHs, and the collision cross section  $\sigma_{pbh,*}$ . Similarly, a reasonable estimate of the collision energetics should depend only on the mass and radius of the star,  $M_*$ ,  $R_*$ , mass of the black hole  $m_{pbh}$ , and the relative velocity  $v_*$ .

The final results obtained this way fully justify the adopted strategy. They show that the hypothetical collisions would be far too infrequent, or far too energetically weak, to be detected. This holds *in the whole range* of  $m_{pbh}$  and all other parameters of the model. The mismatch involves several orders of magnitude. Thus, our conclusion that *there are no observational constraints from*

*hypothetical collisions of hypothetical dark halo primordial black holes with Galactic objects* cannot be changed by including fine details, for example by considering some particular mass functions for  $m_{pbh}$ .

### 3.1. How frequent are the collisions?

Let us consider a spherical part of the Galaxy with the radius  $r$  containing  $N_*(r)$  stars. We will consider stars of a specific type, e.g. main sequence, white dwarf, or neutron star. The dark matter mass in the region is  $M_{DM}(r)$ . The number density of primordial black holes can be estimated by assuming that PBHs represent a fraction  $\eta$  of the dark matter in the region, and that the mass of a single PBH is  $m_{pbh}$  ( $\eta$  and  $m_{pbh}$  are free parameters of the model),

$$n_{pbh}(r) = \frac{\eta \cdot M_{DM}(r)}{4\pi/3 r^3} \cdot \frac{1}{m_{pbh}}. \quad (2)$$

The collision frequency is given by,

$$\dot{n}(r) \approx N_*(r) \cdot j_{pbh}(r) \cdot \sigma_{pbh,*}(r) \approx N_*(r) \cdot \frac{\eta \cdot M_{DM}(r)}{4/3 \pi r^3} \cdot \frac{V(r)}{m_{pbh}} \cdot \sigma_{pbh,*}(r). \quad (3)$$

Here  $\sigma_{pbh,*}$  is the cross section of the interaction, and  $j_{pbh}(r) = n_{pbh}(r) \cdot V(r)$  is the flux of PBHs that move with respect to stars with the relative velocity  $V(r)$ . We approximate  $V(r)$  by the rotational velocity in the Galaxy, which is close to radial.

The cross section  $\sigma_{pbh,*}(r) = \pi R_0^2(r)$  should be calculated from the energy and momentum conservation during the encounter of gravitationally interacting star and PBH. The impact parameter  $R_0(r)$  of the encounter is defined by the PBH angular momentum, equal to

$$m_{pbh} \cdot V(r) \cdot R_0(r). \quad (4)$$

As we are interested in an optimistic estimate of the event rate, and hence of the cross section, here we use the conservation of angular momentum in order to put an upper limit on the impact parameter  $R_0$  for which there is a collision. This means that we use the maximum value for  $R_0$  for each collision, even if this value may be smaller in reality. This maximum value for the impact parameter corresponds to the limiting case of a PBH only grazing the star's surface, so that from angular momentum conservation we get

$$m_{pbh} V(r) R_0 = m_{pbh} v_* R_* \Rightarrow R_0 = R_* \frac{v_*}{V(r)} \quad (5)$$

where  $v_*$  is the final PBH speed, that can be computed by considering energy conservation in the limit of  $m_{pbh} \ll M_*$ :

$$\frac{1}{2} V^2 - \frac{GM_*}{\langle R \rangle} = \frac{1}{2} v_*^2 - \frac{GM_*}{R_*} \quad (6)$$

with  $M_*$  being the mass of the star and  $\langle R \rangle$  being the typical distance between stars. The characteristic distance at which the PBH enters the gravitational field of the star can be approximated

as the typical distance between objects in the Galaxy, assuming that each star-like object deflects the PBH at least marginally. We take this typical distance to be  $\langle R \rangle \sim 1$  pc. We find that the gravitational energy is negligible in the initial state<sup>1</sup>, so that the final velocity can be expressed as

$$v_\star \approx \sqrt{V^2(r) + \frac{2GM_\star}{R_\star}} = \sqrt{V^2(r) + v_{esc}^2}, \quad (7)$$

where  $v_{esc} = 2GM_\star/R_\star$  is the escape velocity of the star. Combining equations (7) and (5) one arrives at

$$R_0(r) = R_\star \cdot \frac{v_\star(r)}{V(r)} = R_\star \cdot \frac{\sqrt{V^2(r) + v_{esc}^2}}{V(r)}. \quad (8)$$

Replacing the impact parameter  $R_0$  in Equ. (3) with the help of Equ. (8) we get, finally

$$\dot{n}(r) \approx N_\star(r) \cdot \frac{\eta \cdot M_{DM}(r)}{4/3 r^3} \cdot \frac{V(r)}{m_{pbh}} \cdot \left( \frac{v_\star(r)}{V(r)} \right)^2 \cdot R_\star^2 \quad (9)$$

Now, the radial dependence of the parameters needs to be specified. The observed velocity profile of the Galaxy can roughly be approximated as  $V(r) = v_0 \cdot r/r_D$  for  $0 < r < r_d \approx 2.5$  kpc, and  $V(r) = v_0$  for  $r_d \leq r < r_{halo} \approx 50$  kpc. Starting from this observational fact, mass densities and masses enclosed in a radius  $r$  can be determined, as listed in table 2. This naturally divides our estimates in a central part, considering only the bulge of the Galaxy, and an outer part, considering the part of the Galaxy where the velocity is constant. Here, we will first consider the outer part of the Galaxy. In Section 3.3, we will show how our results change for the central part.

If the region considered is the whole outer part of the Galaxy (the “flat rotational curve region” outside the bulge), one may use  $r = r_{halo} \sim 50$  kpc,  $M_{DM} \approx 9 \cdot 10^{11} M_\odot$ , and  $V(r) = v_0 \approx 2.2 \cdot 10^7 \text{ cm s}^{-1}$ . Introducing units convenient in this region,  $N_{\star,9} \equiv N_\star/10^9$ ,  $v_{\star,0} \equiv v_\star/v_0$ ,  $R_{\star,9} \equiv R_\star/(10^9 \text{ cm})$  and  $m_{pbh,20} \equiv m_{pbh}/(10^{20} \text{ g})$ , one writes (9) in the form

$$\dot{n} \approx 2 \cdot 10^{-3} \text{ yr}^{-1} \cdot N_{\star,9} \cdot \eta \cdot v_{\star,0}^2 \cdot R_{\star,9}^2 \cdot \left( \frac{v_0}{2.2 \cdot 10^7 \text{ cm/s}} \right) \cdot m_{pbh,20}^{-1}. \quad (10)$$

Apart from the PBH mass (which is a free parameter) this estimate depends only on the stellar properties. For instance, white dwarfs (with  $v_\star/v_0 = 51/2.2$ ) have an event rate of  $1.4 \text{ yr}^{-1}$  for a black hole mass of  $10^{20} \text{ g}$ .

### 3.2. How energetic is a single event?

In estimating the kinetic energy which is transferred from the black hole to the star and then radiated, we follow previous studies of the motion of accretors in a continuous medium, see

---

<sup>1</sup>For  $\langle R \rangle = 1$  pc, we get  $GM_\star/\langle R \rangle \approx 7 \cdot 10^3 \text{ cm s}^{-1}$ . The initial gravitational potential only becomes important for distances below  $\langle R \rangle < 0.01$  pc, where the term  $GM_\star/\langle R \rangle$  becomes comparable to the initial velocity. Since such short distances between stars are rather rare, we neglect this effect. As a comparison, the distance between the Sun and its closest neighbor is  $\sim 1.3$  pc.



e.g. Ruderman and Spiegel (1971). In making this first estimate, we assume a uniform and frictionless medium and disregard self-gravity of the gas.

The black hole passing through the gas focuses matter behind itself, creating a wake, because of the gravitational interaction transferring momentum to the atoms nearby. The inhomogeneity in the medium gives rise to a force acting on the black hole, causing a decrease in kinetic energy.

As pointed out by Ostriker (1999), the force on the black hole (and hence the energy loss) depends on whether the motion is supersonic or not, as well as on the degree of supersonic motion. In making a first order approximation, we consider the black hole to be moving at constant speed. Also, we assume the velocity to be supersonic, so that the drag force, and hence the energy loss, reduces to that given by Ruderman and Spiegel (1971). The energy loss due to the bow shock is negligible compared to that due to the tail shock, and the energy loss per time is then given by

$$\frac{dE_{\text{loss}}}{dt} = \frac{4\pi G^2 m_{pbh}^2 \rho_\star}{v_\star} \ln \frac{D_{\text{max}}}{D_{\text{min}}}, \quad (11)$$

where  $D_{\text{max}}$  is the maximum linear dimension of the star (i.e. its diameter) and  $D_{\text{min}}$  is the linear dimension of the accretor, lying between the black hole's horizon radius and its Bondi-Hoyle accretion radius. The exact formulation of the linear scales is not crucial for this first estimate, as they appear in a logarithm. Here, we use  $\ln(D_{\text{max}}/D_{\text{min}}) = 10$ . The total energy loss is then given by

$$E_{\text{loss}} = \frac{dE_{\text{loss}}}{dt} \cdot dt = \frac{8\pi G^2 m_{pbh}^2 R_\star \rho_\star}{v_\star^2} \ln \frac{D_{\text{max}}}{D_{\text{min}}}, \quad (12)$$

considering a time interval of  $dt \approx 2 \cdot R_\star / v_\star$ . Equation (12) can be expressed as

$$E_{\text{loss}} = 2 \cdot 10^{27} \text{ erg} \cdot m_{pbh,20}^2 \cdot R_{\star,9} \cdot \left( \frac{v_\star}{2.2 \cdot 10^7 \text{ cm/s}} \right)^{-2} \cdot \rho_{\star,5}, \quad (13)$$

where  $\rho_{\star,5} \equiv \rho_\star / (10^5 \text{ g cm}^{-3})$ . Table 3 lists the energy released and the interaction probability for black holes of  $10^{20} \text{ g}$  passing through the different types of Galactic objects.

In our picture, the shock front will locally heat the plasma to an extent depending on the particular Galactic object under consideration. The spectrum is therefore a thermal one. In the following, we discuss the peak energy of the spectrum in order to estimate the detectability for detector systems observing in the relevant energy range.

To calculate the temperature of the shock, we assume supersonic shock conditions and a perfect gas, giving

$$T_S = \frac{5}{64} \frac{m_H}{k_B} v_\star^2 M^2 > 4.5 \cdot 10^5 \text{ K} \cdot \left( \frac{v_\star}{2.2 \cdot 10^7 \text{ cm/s}} \right)^2, \quad (14)$$

where the downstream velocity is diminished by a factor of four with respect to the upstream velocity (see, for example, Landau and Lifshitz (1987); Parks (1991)). Here,  $k_B$  is the Boltzmann constant,  $v_\star$  is the velocity of the shock,  $m_H$  is the mass of a hydrogen atom,  $M$  is the Mach



number, and the average relative velocity between primordial black holes and stars is taken to be  $2.2 \cdot 10^7 \text{ cm s}^{-1}$ . Wien’s law now gives the frequency at maximum intensity as

$$\nu_{\max} = \frac{c T_S}{b} = \frac{c}{b} \cdot \frac{5}{64} \frac{m_H}{k_B} v_*^2 M^2 > 4.5 \cdot 10^{16} \text{ Hz} \cdot \left( \frac{v_*}{2.2 \cdot 10^7 \text{ cm/s}} \right)^2, \quad (15)$$

where  $b = 2.9 \cdot 10^{-3} \text{ Km}$ . This can also be expressed in terms of the peak photon energy

$$E_{\text{peak}} = h \nu_{\max} > 0.2 \text{ keV} \cdot \left( \frac{v_*}{2.2 \cdot 10^7 \text{ cm/s}} \right)^2. \quad (16)$$

This is merely a lower limit, but should suffice as a first-order estimate. For a collision with Earth, an extreme ultraviolet spectrum is expected, while collisions with main sequence stars and red giant cores are expected to give an X-ray spectrum. White dwarfs and neutron stars cannot be treated with simple thermodynamics: we here assume that the shock velocity  $v_*$  determines the temperature of the shock. Thus, we get a peak energy which is increased by a factor  $4^2 = 16$ ,

$$E_{\text{peak}} = 1.6 \text{ keV} \cdot \left( \frac{v_*}{2.2 \cdot 10^7 \text{ cm/s}} \right)^2. \quad (17)$$

For a white dwarf, we get a soft  $\gamma$  spectrum, while for a neutron star we get high-energy gamma rays, see table 3. Since we are dealing with order-of-magnitude estimates here, the actual peak energy could deviate from what is calculated. Therefore, we present our results for all objects and for all possibly interesting energy ranges, i.g. X-rays up to  $\gamma$ -rays.

### 3.3. A scaling to the bulge

The estimates of frequency (9) and energy (12) are general and valid everywhere in the Galaxy. We have already numerically specified them for the region outside the bulge, where the velocity  $v_0 = V(r) = \text{const}$ . We will now discuss them for the central bulge. Note that only the frequency equation (9) contains parameters  $r$ ,  $N_* \approx M_{\text{lum}}/M_\odot$ ,  $M_{DM}$ ,  $v_0$  that depend on the region in the Galaxy. The energy equation (12) does not depend on the relative velocity of stars and PBHs  $v_0$  because the actual velocity of collision  $v_*$  is usually dominated by the escape velocity at the stellar surface.

The frequency equation (9) scales with the relevant parameters as,

$$\dot{n} \sim M_{\text{lum}} M_{DM} r^{-3} v_0^{-1}. \quad (18)$$

Let us now consider a model of the Galaxy in which the rotational velocity  $V(r)$  is proportional to the distance from the Galactic Center in the “bulge” and constant “outside”. This approximately follows what is observed. Distributions of the total (i.e. luminous plus dark matter) mass  $M_{\text{tot}}(r)$  and its density  $\rho(r)$  may be calculated from

$$\frac{V^2}{r} = \frac{d\Phi}{dr}, \quad -4\pi G\rho = \frac{1}{r^2} \frac{d}{dr} \left( r^2 \frac{d\Phi}{dr} \right), \quad \frac{dM_{\text{tot}}}{dr} = 4\pi r^2 \rho. \quad (19)$$

Results are given in Table 2. One may assume that  $M_{lum}(r)M_{DM}(r) \sim M_{tot}^2(r)$ . Then, in the bulge it is  $M_{tot}^2 \sim r^6$ ,  $V(r) \sim r$  and therefore  $\dot{n} \sim r^2$ , which means that in the bulge the frequency of collisions is maximal for  $r = r_D$ ; it does *not* increase towards the bulge center. Let us denote this maximal frequency by  $\dot{n}_D$ , and let us denote the frequency in the outside region by  $\dot{n}_{out}$ . From the above discussion and the last column of Table 2 it follows that,

$$\frac{\dot{n}_D}{\dot{n}_{out}} = \frac{M_D^2 r_D^{-3}}{M_{out}^2 r_{out}^{-3}} = \frac{r_{out}}{r_D} \approx 20. \quad (20)$$

In the view of our estimate at the end of Section 3.1, the collision frequency  $\dot{n}_{out}$  in the outside part of the Galaxy is extremely small. The factor of 20 does change much the situation in the bulge; the collision frequency  $\dot{n}_D$  is also very small there. For this reason, in the rest of this paper we will not distinguish between the outside and the bulge, and take in our estimates of observational detectability  $\dot{n} = \dot{n}_{out}$  as representative for the whole Galaxy.

#### 4. Signatures and detectability of a single encounter

An encounter in which a PBH passes through a stellar object would be detectable if the following conditions are met:

1. *each single event is strong enough to be seen by the detector;*
2. *the events are frequent enough so that they can be seen within the detector's life time.*

In subsection 4.1, we use the sensitivity of current detectors to calculate the maximum distance at which an event could be observed; in subsection 4.2, we estimate the required observation time for a detection. Both estimates are based on the energy loss and event rate calculated in Sections 3.2 and 3.1. In Section 4.3, we determine the actual observation time required in order to see a single event in one of the current detectors.

##### 4.1. Detector sensitivity and photon fluence

The aim of this section is to calculate the maximum distance at which an encounter involving a PBH passing through a Galactic object could be observed by a detector. This can be done by comparing the sensitivity of a detector,  $F_{sens}$ , to the photon fluence from the event,  $F_\gamma$ . Detection is only possible for

$$F_\gamma \geq F_{sens}. \quad (21)$$

The photon fluence and instrumental sensitivity can be determined as follows:

- **Photon fluence from a PBH passing through a Galactic object**

The photon fluence at Earth depends on the total energy deposited as given by Equ. (13)

and on the distance of the event from Earth,  $d$ ,

$$F_\gamma = \frac{E_{\text{loss}}}{\Omega \cdot (1+z) \cdot d^2} \approx \frac{E_{\text{loss}}}{\Omega \cdot d^2} . \quad (22)$$

The redshift factor  $(1+z)$  describes adiabatic energy losses, which can be neglected on Galactic scales,  $z \approx 0$ . The opening angle of the emitted signal  $\Omega$  is determined by the shape of the shock.

- **Sensitivity**

For a positive detection, an instrument with an effective area  $A_{eff}$  needs to see at least one photon of energy  $E_\gamma$ , giving a fluence sensitivity of

$$F_{sens} = \frac{E_\gamma}{A_{eff}} . \quad (23)$$

This assumes that there is no additional background; as soon as there is some significant background, more than one photon would be needed for detection. We use this single photon argument to give an absolute lower limit on the fluence required in order for the signal to be detected.

Combining Equations (21), (22) and (23), we have

$$\frac{E_{\text{loss}}}{\Omega \cdot d^2} \geq \frac{E_\gamma}{A_{eff}} . \quad (24)$$

Typically, the effective detection area  $A_{eff}$  depends on the energy  $E_\gamma$  of detection, and the detector is sensitive to the shape of the spectrum. Here, we optimistically assume that the effective area is concentrated at the lower energy threshold of the detector. For higher energies, the sensitivity would be less. For a given detector, the distance between the detector and the event to be observed must be less than

$$d \leq \sqrt{\frac{E_{\text{loss}}}{E_\gamma} \cdot \frac{A_{eff}}{\Omega}} =: d_{\text{max}} . \quad (25)$$

Inserting into this the expression for the total energy released, as given by Equ. (13), leads to

$$d \leq d_{\text{max}} = 4.7 \text{ pc} \cdot m_{pbh,20} \cdot R_{\star,9}^{1/2} \cdot \left( \frac{v_\star}{2.2 \cdot 10^7 \text{ cm/s}} \right)^{-1} \cdot \rho_{\star,5}^{1/2} \cdot A_{eff,2500}^{1/2} \cdot \Omega_{2\pi}^{-1/2} \cdot E_{\gamma,1.5}^{-1/2} , \quad (26)$$

where values are given in terms of the X-ray detector XMM Newton: the effective area reference value is  $A_{eff,2500} \equiv A_{eff}/(2500 \text{ cm}^2)$ , at a reference energy of  $E_{\gamma,1.5} \equiv E_\gamma/(1.5 \text{ keV})$ . The opening angle of the signal is expressed in terms of the maximum opening angle, corresponding to a signal emitted over half a hemisphere,  $\Omega_{2\pi} \equiv \Omega/(2\pi)$ .

#### 4.2. Observation time and interaction probability

We can evaluate the observation time  $t_{obs}$  required for detecting the effect of a PBH passing through a Galactic object, by considering the event rate within the observable distance  $d_{\max}$ ,  $\dot{n}(d_{\max})$ . The latter can be calculated from the total event rate,  $\dot{n}$ , as calculated in Section 3.1:

$$\dot{n}(d_{\max}) = \frac{V(d_{\max})}{V_{tot}} \cdot \dot{n}, \quad (27)$$

where,  $V(d_{\max})$  is the volume containing the observable events

$$V(d_{\max}) = \pi d_{\max}^2 h \quad (28)$$

and

$$V_{tot} = \pi d_{\text{Galaxy}}^2 h, \quad (29)$$

with  $d_{\text{Galaxy}} \approx 15$  kpc being the radius of the Galaxy. We assume an isotropic distribution of sources within the Galactic disk with a height  $h = 300$  pc. This means that we assume that the signal is always strong enough to reach Earth from 300 pc across the height of the disk. Realistically, some signals will be lost, since they are too weak to be detected at Earth, but as mentioned before, we work with the most optimistic assumptions in this paper.

The number of events occurring within the observable distance  $d_{\max}$  from Earth is given as:

$$N = \dot{n}(d_{\max}) \cdot \frac{\Omega_{obs}}{4\pi} \cdot \frac{\Omega}{4\pi} \cdot t_{obs}. \quad (30)$$

In this equation, the solid angle  $\Omega_{obs}$  describes the Field of View (FoV) of the detector. The solid angle  $\Omega$  accounts for a possibly beamed signal, which reduces the total number of events to be observed, since only a fraction  $\Omega/(4\pi)$  is directed towards Earth. The total event rate  $\dot{n}$  in the Galaxy was determined in Section 3.1.

Using Equations (27), (28) and (29) in Equ. (30), the number of events within a radius  $d_{\max} \leq d_{\text{Galaxy}}$  is given as

$$N = \dot{n} \cdot \left( \frac{\min(d_{\max}, d_{\text{Galaxy}})}{d_{\text{Galaxy}}} \right)^2 \cdot \frac{\Omega_{obs}}{4\pi} \cdot \frac{\Omega}{4\pi} \cdot t_{obs}. \quad (31)$$

The radius of the Galaxy  $d_{\text{Galaxy}}$  gives an absolute limit for the number of events. For detection of a single event ( $N = 1$ ), the required observation time is then

$$t_{obs} = 1 \text{ yr} \cdot \frac{4\pi}{\Omega_{obs}} \cdot \frac{4\pi}{\Omega} \cdot \left( \frac{\dot{n}}{1 \text{ yr}^{-1}} \right)^{-1} \cdot \left( \frac{\min(d_{\max}, d_{\text{Galaxy}})}{d_{\text{Galaxy}}} \right)^{-2}. \quad (32)$$

Combining Equations (9), (26) and (32) gives

$$\begin{aligned} t_{obs}(m_{pbh} < m_{pbh}^{\text{break}}) = 7.0 \cdot 10^{11} \text{ yr} & \cdot m_{pbh,20}^{-1} \cdot R_{\star,9}^{-3} \cdot \rho_{\star,5}^{-1} \cdot N_{\star,9}^{-1} \cdot \Omega_{2\pi}^{-1} \\ & \cdot \eta^{-1} \cdot A_{eff,2500}^{-1} \cdot \Omega_{obs,0.2}^{-1} \cdot E_{\gamma,1.5} \end{aligned} \quad (33)$$

for  $d_{\max} < d_{\text{Galaxy}}$  and

$$t_{\text{obs}}(m_{\text{pbh}} \geq m_{\text{pbh}}^{\text{break}}) = 1 \cdot 10^3 \text{ yr} \cdot \Omega_{\text{obs},0.2}^{-1} \cdot \Omega_{2\pi}^{-1} \cdot N_{\star,9}^{-1} \cdot \eta^{-1} \cdot m_{\text{pbh},20} \cdot v_{\star,0}^{-2} \cdot R_{\star,9}^{-2} \cdot \left( \frac{v_0}{2.2 \cdot 10^7 \text{ cm/s}} \right)^{-1} \quad (34)$$

for  $d_{\max} = d_{\text{Galaxy}}$ . Here,  $\Omega_{\text{obs},0.2} \equiv \Omega_{\text{obs}}/(0.2 \text{ sr})$ .

This break in the function  $t_{\text{obs}}(m_{\text{pbh}})$  occurs at a mass of

$$m_{\text{pbh}}^{\text{break}} = 3.2 \cdot 10^{23} \text{ g} \cdot R_{\star,9}^{-1/2} \cdot \left( \frac{v_{\star}}{2.2 \cdot 10^7 \text{ cm/s}} \right) \cdot \rho_{\star,5}^{-1/2} \cdot \Omega_{2\pi}^{1/2} \cdot A_{\text{eff},2500}^{-1/2} \cdot E_{\gamma,1.5}^{1/2}. \quad (35)$$

The observation time reaches its minimum at this break mass. At lower masses up to the break mass,  $m_{\text{pbh}} \leq m_{\text{pbh}}^{\text{break}}$ , the observation time follows a  $m_{\text{pbh}}^{-1}$  behavior. At higher masses,  $m_{\text{pbh}} > m_{\text{pbh}}^{\text{break}}$ , the observation time increases as  $m_{\text{pbh}}^2$ . Observation conditions are therefore optimal at the break mass.

### 4.3. Detectability

As discussed in Section 3.2, the signals are expected to come at X-ray energies. We focus here on four detectors currently in operation which are well-suited for these investigations because of their relatively large FoVs and effective areas. First we consider XMM NEWTON which is sensitive from extreme UV to X-rays. We use its effective area as quoted in Aschenbach (2002) at the reference energy 1.5 keV. The results which we obtain for this are equivalent to what is expected for observations with Chandra. For higher energies, from hard X-rays to soft gamma-rays, we use SWIFT-BAT and FERMI-GBM as reference detectors. Swift covers the range between 15 keV and 150 keV; the high-energy detector of the GBM covers the energy range from 150 keV to 30 MeV. Both instruments provide quite large effective areas in combination with a large FoV, since they were designed to detect GRBs. For high-energy radiation, we use Fermi-LAT parameters, covering the range from 20 MeV up to 300 GeV. Table 4 summarizes the properties of the four detectors. For Swift and Fermi, we use the lower energy thresholds as the reference energies for the effective areas quoted in (Barthelmy et al. 2005; Meegan et al. 2008; Michelson 2003). This is the most optimistic approach, since using higher energies would lead to reduced sensitivities.

The detector’s effective area, FoV and reference energy then determine the observation time and the break masses as discussed in the previous subsection. It turns out that the observation times for the four different detectors are related as

$$t_{\text{obs}}^{\text{XMM}} = 2 \cdot t_{\text{obs}}^{\text{Swift/BAT}} = 0.2 \cdot t_{\text{obs}}^{\text{Fermi/GBM}} = 0.003 \cdot t_{\text{obs}}^{\text{Fermi/LAT}} \quad (36)$$

and the break masses  $m_{\text{pbh}}^{\text{break}}$  are related as

$$m_{\text{pbh}}^{\text{break,XMM}} = 2 \cdot m_{\text{pbh}}^{\text{break,Swift/BAT}} = 0.1 \cdot m_{\text{pbh}}^{\text{break,Fermi/GBM}} = 0.02 \cdot m_{\text{pbh}}^{\text{break,Fermi/LAT}}. \quad (37)$$

Swift/BAT gives the shortest observation time and is therefore best option concerning this. Fermi/LAT gives the largest break mass. Figure 2 shows observation time plotted against PBH mass for the case of XMM Newton in the relevant mass range of  $10^{15} \text{ g} < m_{pbh} < 10^{26} \text{ g}$ . Masses outside this range are already known not to contribute significantly ( $< 10\%$ ) to the dark matter. The solid line represents main sequence stars, the dashed line shows red giant cores, the dotted line is the result for white dwarfs and the dot-dashed line is for neutron stars. The shortest observation times are obtained for main sequence stars, and even there, the best case at  $m_{pbh} = 2 \cdot 10^{24} \text{ g}$  requires an observation time of more than 100 years. Similar results are obtained for Swift, Fermi-GBM and Fermi-LAT, as shown in Figures 3, 4 and 5: here as well, the observation times would need to be longer than 100 years in order to see one event, except in the case of Fermi/GBM at  $3 \cdot 10^{25} \text{ g}$ , where 60 years would be sufficient. The best observation times  $t_{obs}^{best}$  are those for the break points in the plots of the observation time against PBH mass  $m_{pbh}^{break}$ . They are listed for the four detectors in Table 4.

These observation times are far longer than the lifetimes of the present detectors and so, given that they are anyway optimistic lower limits on the real times, we conclude that we cannot obtain meaningful constraints in this way. The event rates are too low and the energy released is too small.

Any constraint which we could give for the PBH contribution to dark matter in the Galaxy would be above 100%. We therefore do not convert the observation times into limits on the dark matter contribution.

#### 4.4. Alternative signatures

There are a few other processes that could in principle lead to the production of a detectable signal for different detectors. We will briefly discuss here why these mechanisms also fail to produce a significant signal:

- *Shock acceleration of charged particles*

Particles can gain energy by scattering off magnetic inhomogeneities via the mechanism of stochastic acceleration (Fermi 1949, 1954). However, inside stars the densities are typically very high, and for white dwarfs and neutron stars the matter is degenerate. The mean free path of a proton in matter can be determined by considering the total cross section for proton-proton interactions (with  $\sigma_{pp} \approx 50 \text{ mbarn}$ ):

$$\lambda_{mfp} = \frac{m_p}{\rho_{\star} \cdot \sigma_{pp}} = 3 \cdot 10^{-4} \text{ cm} \cdot \rho_{\star,5} . \quad (38)$$

This mean free path is typically smaller than a centimeter and does not allow for significant acceleration. Injection and acceleration of energetic charged particles in shock fronts is therefore highly disfavored, with the possible exception of the tenuous envelopes of red giant stars.

- *Star quakes*

PBHs passing through an astrophysical object can induce star quakes. Although the emitted photons themselves cannot be distinguished from the general thermal spectrum of the star, the event could be detected by Fourier-transforming the spectrum from time to frequency space, see (Donea et al. 1999; Martínez-Oliveros et al. 2007, e.g.) and references therein. However, these quakes can so far only be detected for the Sun and our rate for encounters between a PBH and the Sun is only  $10^{-7} \text{ yr}^{-1}$ . This method for getting detections can therefore be excluded.

## 5. On the possibility of a PBH being captured by a star

Roncadelli et al. (2009) have considered the possibility of a PBH being captured by a star. In this section, we show that such a capture could happen only for PBHs with masses greater than about  $10^{28} \text{ g}$ , i.e. in the range already constrained by the micro-lensing results discussed earlier. The capture rates would therefore be reduced by a factor of 10 or more, considering that  $\eta < 0.1$ .

The energy balance for a PBH being attracted by an astrophysical object in the formulation of a reduced two-body problem is given by

$$E_{\text{in}} - E_{\text{loss}} = E_{\text{out}}. \quad (39)$$

Here,  $E_{\text{loss}}$  is the energy loss undergone by the PBH as it passes through the star and  $E_{\text{out}}$  is its final energy. Its initial energy is given by

$$E_{\text{in}} = \frac{1}{2} \cdot m_{pbh} \cdot v_0^2, \quad (40)$$

where we replace the reduced two-body mass by  $m_{pbh}$ , because we are considering  $M_\star \gg m_{pbh}$ . The PBH can be captured by the star only if a sufficient part of its initial kinetic energy can be dissipated (“lost”) by the effective dynamical friction as it passes through the star. The condition for getting a bound system is  $E_{\text{out}} < 0$ . From Equations (39) and (40) we get

$$E_{\text{loss}} > E_{\text{in}} = \frac{1}{2} \cdot m_{pbh} \cdot v_0^2. \quad (41)$$

This is the condition that needs to be fulfilled in order to have a capture. The energy loss from effective friction should be dominant, as determined from Equ. (12). It follows that

$$\frac{2 E_{\text{loss}}}{m_{pbh}} = 4 \cdot 10^7 \frac{\text{cm}^2}{\text{s}^2} \cdot m_{pbh,20} \cdot \left( \frac{v_\star}{2.2 \cdot 10^7 \text{cm/s}} \right)^{-2} \cdot R_{\star,9} \cdot \rho_{\star,5} \stackrel{(\text{Equ. 41})}{>} v_0^2. \quad (42)$$

We can now derive a condition for the minimum PBH mass required for capture:

$$m_{pbh,20} > \left( \frac{v_0}{2.2 \cdot 10^7 \text{cm/s}} \right)^2 \cdot \left( \frac{v_{\text{esc}}^2 + v_0^2}{4 \cdot 10^7 \text{cm}^2/\text{s}^2} \right) \cdot R_{\star,9}^{-1} \cdot \rho_{\star,5}^{-1} \quad (43)$$

$$> \left( \frac{v_0}{2.2 \cdot 10^7 \text{cm/s}} \right)^2 \cdot \left( 6.6 \cdot 10^9 \cdot M_{\star,\odot} \cdot R_{\star,9}^{-1} + 1.2 \cdot 10^7 \cdot \frac{v_0^2}{(2.2 \cdot 10^7 \text{cm/s})^2} \right) \cdot R_{\star,9}^{-1} \cdot \rho_{\star,5}^{-1} \quad (44)$$



The minimum mass for which capture can occur can now be computed for each of the astrophysical objects which we are considering (see table 3):

$$m_{pbh} > 6.6 \cdot 10^{28} \text{ g} \cdot \frac{v_0^2}{(2.2 \cdot 10^7 \text{ cm/s})^2} + 1.2 \cdot 10^{28} \text{ g} \cdot \frac{v_0^4}{(2.2 \cdot 10^7 \text{ cm/s})^4} \quad \text{main seq. stars,} \quad (45)$$

$$m_{pbh} > 6.6 \cdot 10^{28} \text{ g} \cdot \frac{v_0^2}{(2.2 \cdot 10^7 \text{ cm/s})^2} + 1.2 \cdot 10^{27} \text{ g} \cdot \frac{v_0^4}{(2.2 \cdot 10^7 \text{ cm/s})^4} \quad \text{RGCs,} \quad (46)$$

$$m_{pbh} > 6.6 \cdot 10^{29} \text{ g} \cdot \frac{v_0^2}{(2.2 \cdot 10^7 \text{ cm/s})^2} + 1.2 \cdot 10^{27} \text{ g} \cdot \frac{v_0^4}{(2.2 \cdot 10^7 \text{ cm/s})^4} \quad \text{white dwarfs,} \quad (47)$$

$$m_{pbh} > 6.6 \cdot 10^{27} \text{ g} \cdot \frac{v_0^2}{(2.2 \cdot 10^7 \text{ cm/s})^2} + 1.2 \cdot 10^{22} \text{ g} \cdot \frac{v_0^4}{(2.2 \cdot 10^7 \text{ cm/s})^4} \quad \text{neutron stars.} \quad (48)$$

On the view that the existence in the dark halo of PBHs with masses greater than about  $10^{26}$  g is already constrained by the micro-lensing observations, we conclude that the capture of a PBH by a star is difficult in *any* of the PBH mass ranges. Only relative velocities far below the average value could lead to a capture, but such events do not happen often enough to be significant. If any PBHs are captured by stars, this must be extremely rare, and certainly the fact that we do not observe them does not additionally constrain the PBH abundance in the dark halo of our Galaxy<sup>2</sup>.

The above conclusion follows from the estimate of the energy lost when a PBH passes through a star,  $E_{\text{loss}}$ , based on the Ruderman-Spiegel effective dynamical friction formula. This may explain the difference between our conclusions and those of Roncadelli et al. (2009): they do not estimate  $E_{\text{loss}}$ , but instead assume that any PBH which collides with a star would be captured.

We will examine the problem of estimating the probability of very low velocity PBH-star collisions at high PBH masses in a separate publication.

## 6. Conclusions

We have shown in the previous sections that the process of effective friction when a PBH passes through a Galactic object cannot lead to a significantly detectable signal with current instruments. We calculated lower limits for the observation time for the best-suited detectors: XMM Newton, Swift-BAT, and Fermi-GBM and Fermi-LAT. These lower limits were based on the assumptions that

- *The entire energy loss is radiated without significant delays and at the wavelength at which it is produced,*

---

<sup>2</sup>A few years ago, Bohdan Paczynski suggested in a private conversation with M.A.A., that some unusual and very rare supernova-like events might be due to PBH collisions with white dwarfs. This suggestion was discussed later with Piero Madau, Rashid Sunyaev and others, but never followed up in detail.

- *one photon is sufficient for having a significant detection of a signal,*
- *all emitted energy is contained in the energy range of the detector,*
- *the entire thickness of the Galactic disk can be observed,*
- *the signal is emitted at the largest opening angle, i.e.  $2\pi$ .*

All of these assumptions were made in the sense of favoring detection; more realistic settings would reduce the detectability even more. We have investigated interactions with main sequence stars, red giants, white dwarfs, and neutron stars. In general, we can conclude that the best results are obtained for main sequence stars. However, independently of the class of objects, the difficulty is that either the total energy loss in the process is too small (for lower masses around  $10^{15} \text{ g} < m_{pbh} < 10^{20} \text{ g}$ ) or the event rate is too small (for larger masses around  $10^{20} \text{ g} < m_{pbh} < 10^{26} \text{ g}$ ). Even with the optimistic assumptions listed above, observation times of more than 100 years are required in order to see a single event for all of the objects and all of the detectors considered.

Although we use average values in place of the mass and velocity distributions of PBHs, variations away from these central values will not influence the result of these calculations significantly. One could, for instance, argue that the clumping of dark matter as discussed by Binney and Tremaine (2008) would lead to an enhanced signal. However, such an effect would need to increase the event rate by at least a factor of  $10^2$  in order to achieve reasonable observation times of  $t_{obs} < 1 \text{ yr}$ . As shown in this paper, the central bulge of the Galaxy may improve the situation by a factor of 20, but this is still not enough to reduce observation times to realistic scales of less than a month.

Hence, we conclude that constraining the abundance of PBHs in DM using interactions of PBHs with Galactic objects is not possible in the standard scenario described above. A significant rate of GRB-like events as suggested in (Zhilyaev 2007) can therefore be excluded. There may be additional aspects, such as clumping of dark matter or observation of nearby dwarf galaxies, leading to an enhanced event rate and energy release. However, these will have to be able to improve the observation times in this standard scenario by at least a factor of 100 in order to give a significant signal. The main reason is that observation times of less than a month may be available with the different instruments, but not more.

Concerning a possible collision with the Earth: the predicted rate is as low as  $10^{-12} \text{ yr}^{-1} \cdot m_{pbh,20}^{-1}$ . This means that there would be less than one such event per  $10^{12 \rightarrow 17}$  years for PBH masses above  $10^{20} \text{ g}$ . The interpretation of the Tunguska event as a collision with a PBH of  $m_{pbh} > 10^{20} \text{ g}$ , see Jackson and Ryan (1973), can therefore be considered highly implausible on the basis of this straightforward statistical argument. The most common explanation discussed today is that a comet or asteroid disintegrated on its way to Earth. Since no macroscopic fragments of the initial object were found, its exact nature, comet or asteroid, is still unknown, see e.g. (Jopek et al. 2008).

On the other hand, PBHs with masses below  $m_{pbh} < 10^{17} \text{ g}$  may have struck or could still strike the Earth, as the encounter frequency may be greater than once during the Earth's life time. However,

the energy loss is too small to see such events by means of radiation. The possibility of detecting them by means of an acoustic signal has been discussed by Khriplovich et al. (2008) but there it was pointed out that the signal is too weak to be seen by seismic detectors. It could be interesting to look for those signatures with the planned generation of high-energy neutrino telescopes, optimized to detect acoustic signals: large natural water, ice or salt reservoirs are to be instrumented to look for acoustic signals from Cherenkov radiation, see e.g. (Vandenbroucke 2007; Becker 2008) for a review. The surface area of such a detector is planned to be of the order of  $10 \text{ km}^2$ . If the PBH has a distinct signature, it might be observable with such an instrument.

We would like to thank Wlodek Bednarek, Alina Donea, Maxim Khlopov, John Miller, Wolfgang Rhode and Alessandro Romeo for helpful discussions. MAA acknowledges support from the Polish Ministry of Science, grant N203 0093/1466, and from the Swedish Research Council, grant VR Dnr 621-2006-3288. JKB is supported by the Deutsche Forschungsgemeinschaft (DFG), grant BE-3712/3-1. Support for work with PLB has come from the AUGER membership and theory grant 05 CU 5PD 1/2 via DESY/BMBF and from VIHROS. AG acknowledges support from the Knut and Alice Wallenberg Foundation. For LQ, support is coming from the Chinese Scholarship Council. Further acknowledgments go to Nordita for traveling grants for MAA, JKB and FJ.

## REFERENCES

- C. Afonso et al. *A&A*, 400:951, 2003.
- C. Alcock et al. *Astroph. Journal Let.*, 499:L9, 1998.
- C. Amsler, Particle Data Group, et al. *Phys. Lett. B*, 667:1, 2008.
- B. Aschenbach. In P. Gorenstein and R. B. Hoover, editors, *Society of Photo-Optical Instrumentation Engineers (SPIE) Conference Series*, volume 4496 of *Society of Photo-Optical Instrumentation Engineers (SPIE) Conference Series*, page 8, 2002.
- A. Barrau, G. Boudoul, and L. Derome. In *International Cosmic Ray Conference*, volume 3 of *International Cosmic Ray Conference*, page 1697, 2003.
- S. D. Barthelmy et al. *Space Science Reviews*, 120:143, 2005.
- J. K. Becker. *Phys. Rep.*, 458:173, 2008.
- J. D. Bekenstein. *Phys. Rev. D*, 12:3077, 1975.
- G. Bertone, D. Hooper, and J. Silk. *Phys. Rep.*, 405:279, 2005.
- P. L. Biermann and A. Kusenko. *Phys. Rev. Let.*, 96(9):091301, 2006.

- J. Binney and S. Tremaine. *Galactic Dynamics: Second Edition*. Princeton University Press, Princeton, NJ USA, 2008.
- B. J. Carr. *ArXiv:astro-ph/0504034 (preprint)*, 2005.
- A.-C. Donea, D. C. Braun, and C. Lindsey. *Astroph. Journal Let.*, 513:L143, 1999.
- E. Fermi. *Phys. Rev.*, 75(8):1169, 1949.
- E. Fermi. *ApJ*, 119:1, 1954.
- A. Gould. *Astroph. Journal Let.*, 386:L5, 1992.
- H. E. Haber and G. L. Kane. *Phys. Rep.*, 117:75, 1985.
- F. Halzen et al. *Nature*, 353:807, 1991.
- S. W. Hawking. *MNRAS*, 152:75, 1971.
- S. W. Hawking. *Nature*, 248:30, 1974.
- D. Hooper and S. Profumo. *Phys. Rep.*, 453:29, 2007.
- A. A. Jackson and M. P. Ryan. *Nature*, 245:88, 1973.
- T. J. Jopek et al. *Earth Moon and Planets*, 102:53, 2008.
- F. D. Kahn and L. Woltjer. *ApJ*, 130:705, 1959.
- M. Y. Khlopov. *ArXiv:0801.0116 (preprint)*, 2008.
- I. B. Khriplovich et al. *Phys. Rev. D*, 77(6):064017, 2008.
- E. Komatsu et al. *ApJS*, 180:330, 2009.
- L. D. Landau and E. M. Lifshitz. *Course of Theoretical Physics, Vol.6 : Fluid Mechanics*. Butterworth-Heinemann, 2nd edition, 1987.
- J. C. Martínez-Oliveros et al. *Solar Physics*, 245:121, 2007.
- C. Meegan et al. In M. Galassi, D. Palmer, and E. Fenimore, editors, *American Institute of Physics Conference Series*, volume 1000 of *American Institute of Physics Conference Series*, page 573, 2008.
- P. F. Michelson. In J. E. Trümper and H. D. Tananbaum, editors, *Society of Photo-Optical Instrumentation Engineers (SPIE) Conference Series*, volume 4851 of *Society of Photo-Optical Instrumentation Engineers (SPIE) Conference Series*, page 1144, 2003.
- E. C. Ostriker. *ApJ*, 513:252, 1999.

- J. P. Ostriker, P. J. E. Peebles, and A. Yahil. *Astroph. Journal Let.*, 193:L1, 1974.
- G. K. Parks. *Physics of space plasmas*. Addison-Wesley Publishing Company, 1991.
- M. Ricotti, J. P. Ostriker, and K. J. Mack. *ApJ*, 680:829, 2008.
- M. Roncadelli, A. Treves, and R. Turolla. *ArXiv:0901.1093*, 2009. submitted to PRL.
- M. A. Ruderman and E. A. Spiegel. *ApJ*, 165:1, 1971.
- P. Sreekumar et al. *ApJ*, 494:523, 1998.
- Swift-web. <http://swift.gsfc.nasa.gov/docs/swift/swiftsc.html>, 2008. Swift web-page.
- J. Vandenbroucke. *J.Phys.Conf.Ser*, 60:101, 2007.
- X. X. Xue et al. *ApJ*, 684:1143, 2008.
- J. Yoo, J. Chaname, and A. Gould. *A&A*, 601:311, 2004.
- B. E. Zhilyaev. *Bulletin Crimean Astrophysical Observatory*, 103:58, 2007. arXiv:0706.0930.
- F. Zwicky. Die Rotverschiebung von extragalaktischen Nebeln. *Helvetica Physica Acta*, 6:110, 1933.
- F. Zwicky. *ApJ*, 86:217, 1937.

---

This preprint was prepared with the AAS L<sup>A</sup>T<sub>E</sub>X macros v5.2.

Table 1. Basic properties of objects considered for collisions with primordial black holes.

	Earth	main sequ. stars	red giant cores	white dwarfs	neutron stars
number in MW $N_{\star}$	1	$10^{11}$	$10^9$	$10^9$	$10^9$
mass $M_{\star}/M_{\odot}$	$3 \cdot 10^{-6}$	1	1	1	1
radius $R_{\star}$ [cm]	$6.4 \cdot 10^8$	$10^{11}$	$10^{10}$	$10^9$	$10^6$
density $\rho_{\star}$ [g cm <sup>-3</sup> ]	5.5	100	$10^{4 \rightarrow 5}$	$10^{5 \rightarrow 6}$	$10^{13 \rightarrow 15}$

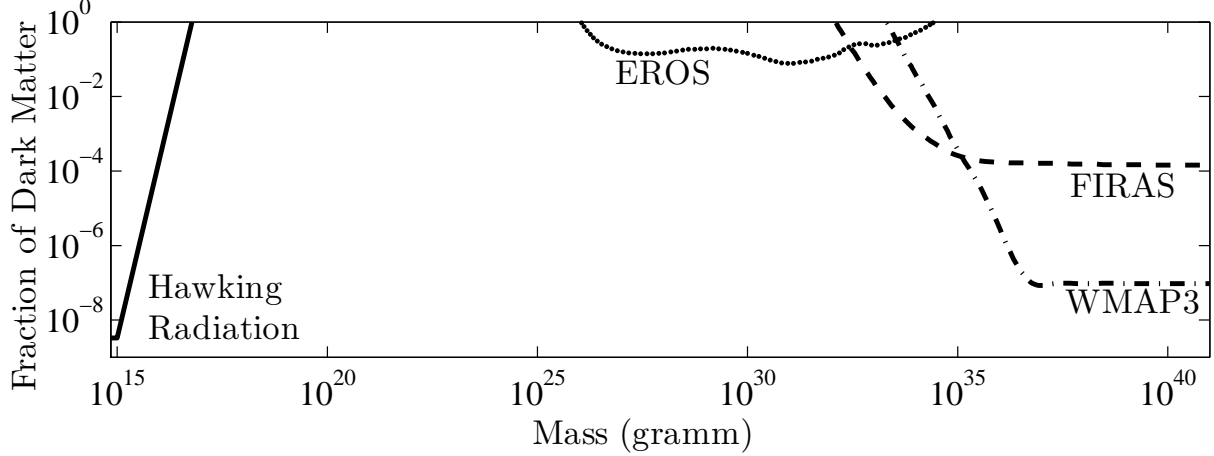


Fig. 1.— Limits on the contribution to dark matter by PBHs. An absolute lower limit at around  $10^{15}$  g is given by the fact that PBHs with lower masses have evaporated by now. The limit at  $\sim 10^{15}$  g is derived from the background of photons at  $> 100$  MeV in the Universe, see (Sreekumar et al. 1998; Barrau et al. 2003). Micro-lensing constraints in the mass range  $10^{26}$  g  $< m_{pbh} < 10^{33}$  g, come from the EROS experiment (Alcock et al. 1998). Limits in the mass range  $10^{33}$  g  $< m_{pbh} < 10^{40}$  g, derived from measurements of the Cosmic Microwave Background by FIRAS and WMAP, are presented in Ricotti et al. (2008). In this figure, we only show the most stringent limits in the different mass regions and disregard those limits with weaker constraints.

Table 2. Basic dependence of the velocity  $V(r)$ , the mass density  $\rho(r)$  and the mass  $M_{tot}(r)$  on the distance from the Galactic Center  $r$ . Here,  $M_{tot}(r)$  denotes the mass enclosed in the volume of the radius  $r$ . The parameters have different dependencies in the outer part of the Galaxy (“outside”) and the central part (“Bulge”).

		$V(r)$	$\rho(r)$	$M_{tot}(< r)$	total enclosed mass
Bulge	$0 < r < r_D$	$(v_0/r_D) r$	$(v_0^2 \cdot r_D/G)$	$(v_0^2 \cdot r_D/G) r^3$	$v_0^2 \cdot r_D/G$
Outside	$r_D < r < r_{halo}$	$(v_0)$	$(v_0^2/(4\pi G)) \cdot r^{-2}$	$(v_0^2/G) \cdot r$	$v_0^2 \cdot r_{halo}/G$

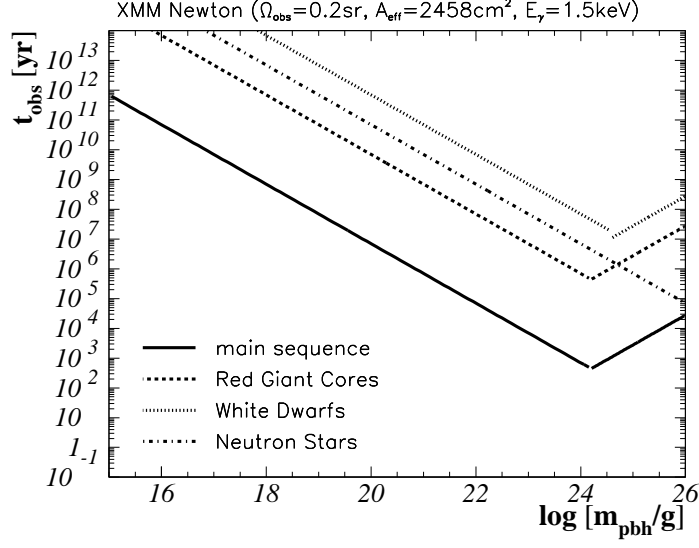


Fig. 2.— Observation time of PBH interactions with Galactic objects, observing with XMM Newton. Solid line: main sequence stars; dashed line: red giant cores; dotted line: white dwarfs; dot-dashed line: neutron stars. The observation time decreases with  $m_{\text{pbh}}^{-1}$ , until the point where the entire Galaxy can be observed, beyond which it starts increasing with  $m_{\text{pbh}}$ .

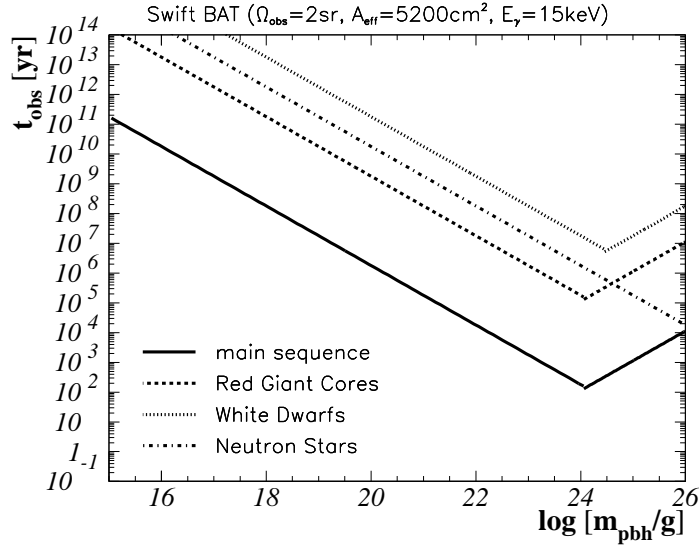


Fig. 3.— Observation time of PBH interactions with Galactic objects, observing with Swift-BAT. Same representation as in Fig. 2.



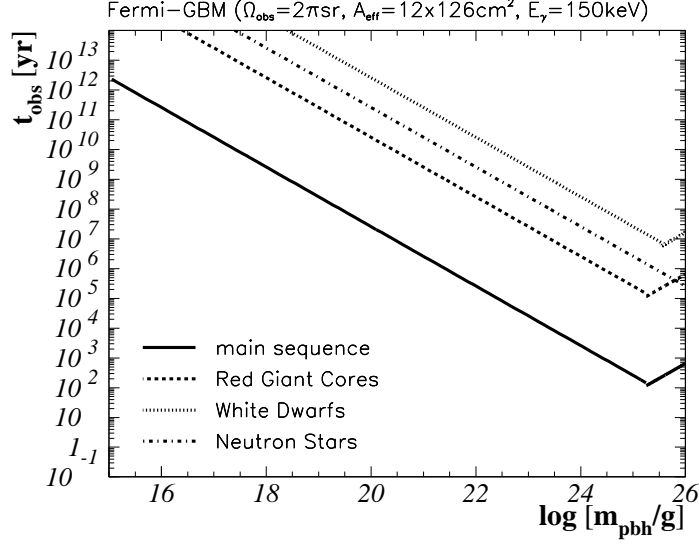


Fig. 4.— Observation time of PBH interactions with Galactic objects, observing with Fermi-GBM. Same representation as in Fig. 2.

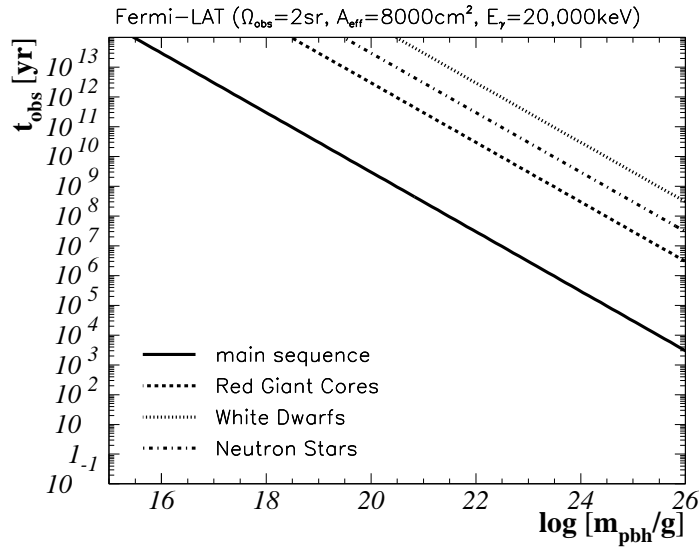


Fig. 5.— Observation time of PBH interactions with Galactic objects, observing with Fermi-LAT. Same representation as in Fig. 2.

Table 3. Energy loss as calculated in Section 3.2, Equ. (13) for a PBH mass of  $m_{pbh} = 10^{20}$  g. The velocity of the PBH at the surface of the star  $v_*$  is calculated according to Equ. (7). The energy loss rate,  $dE_{\text{loss}}/dt$  and the total energy loss  $E_{\text{loss}}$ , scale as  $(m_{pbh}/10^{20}\text{g})^2$ . The time it takes for the PBH to traverse the star is given by  $dt$ , see Section 3.2. The peak energy  $E_{\text{peak}}$  is derived following Equ. (16) in the case of regular stellar objects, and using Equ. (17) for the relativistic objects (neutron stars and white dwarfs). The interaction probability  $\dot{n}$  scales as  $(m_{pbh}/10^{20}\text{g})^{-1}$  according to Equ. (9).

$m_{pbh} = 10^{20}$ g	Earth	main sequ. stars	red giant cores	white dwarfs	neutron stars
$v_*$ [cm s <sup>-1</sup> ]	$2.2 \cdot 10^7$	$5.5 \cdot 10^7$	$1.6 \cdot 10^8$	$5.1 \cdot 10^8$	$1.6 \cdot 10^{10}$
$dE_{\text{loss}}/dt$ [erg s <sup>-1</sup> ]	$1.5 \cdot 10^{21}$	$10^{22}$	$3 \cdot 10^{23 \rightarrow 24}$	$10^{24 \rightarrow 25}$	$3 \cdot 10^{30 \rightarrow 32}$
$dt$ [s]	60	3600	120	3.9	$1.2 \cdot 10^{-4}$
$dE_{\text{loss}}/dt \cdot dt$ [erg]	$9 \cdot 10^{22}$	$4 \cdot 10^{25}$	$4 \cdot 10^{25 \rightarrow 26}$	$4 \cdot 10^{24 \rightarrow 25}$	$4 \cdot 10^{26 \rightarrow 28}$
$E_{\text{peak}}$ [keV]	0.2	1	11	1600	$1.6 \cdot 10^6$
$\dot{n}$ [yr <sup>-1</sup> ]	$8 \cdot 10^{-13}$	$1.3 \cdot 10^4$	11	1.4	$1.1 \cdot 10^{-3}$

Table 4. Detector properties in the X-ray to soft gamma-ray range. In order to give an upper limit on the sensitivity, the lower energy threshold is used as  $E_\gamma$  in the case of Swift and Fermi. For XMM Newton, the reference energy  $E_\gamma = 1.5$  keV was explicitly given for the listed effective area.

	XMM Newton (Aschenbach 2002)	Swift BAT (Swift-web)	Fermi GBM (Meegan et al. 2008)	Fermi LAT (Michelson 2003)
$E_{\text{min}}; E_{\text{max}}$ [keV]	(0.1; 15)	(15; 150)	(10; $3 \cdot 10^4$ )	( $2 \cdot 10^4$ ; $3 \cdot 10^8$ )
$E_\gamma$ [keV]	1.5	15	150	$2 \cdot 10^4$
$\Omega_{\text{obs}}$ [sr]	0.20	2	$\sim 2\pi$	2
$A_{\text{eff}}$ [cm <sup>2</sup> ]	2485	5200	$12 \times 126$	$8 \cdot 10^3$
main seq. stars				
$m_{pbh}^{\text{break}}$ [g]	$2.1 \cdot 10^{24}$	$0.7 \cdot 10^{24}$	$2.1 \cdot 10^{25}$	$1.4 \cdot 10^{26}$
$t_{\text{obs}}^{\text{best}}$ [yr]	280	280	180	1500
Red Giant Cores				
$m_{pbh}^{\text{break}}$ [g]	$2.1 \cdot 10^{24}$	$0.7 \cdot 10^{24}$	$2.1 \cdot 10^{25}$	$1.4 \cdot 10^{26}$
$t_{\text{obs}}^{\text{best}}$ [yr]	$2.8 \cdot 10^5$	$2.8 \cdot 10^5$	$1.2 \cdot 10^5$	$1.5 \cdot 10^6$
White Dwarfs				
$m_{pbh}^{\text{break}}$ [g]	$4.2 \cdot 10^{24}$	$2.1 \cdot 10^{24}$	$4.2 \cdot 10^{25}$	$2.8 \cdot 10^{26}$
$t_{\text{obs}}^{\text{best}}$ [yr]	$1.0 \cdot 10^7$	$1.1 \cdot 10^7$	$4.8 \cdot 10^6$	$7.6 \cdot 10^7$
Neutron Stars				
$m_{pbh}^{\text{break}}$ [g]	$2.1 \cdot 10^{26}$	$7.1 \cdot 10^{25}$	$2.1 \cdot 10^{27}$	$1.4 \cdot 10^{28}$
$t_{\text{obs}}^{\text{best}}$ [yr]	$2.8 \cdot 10^4$	$2.8 \cdot 10^4$	$1.2 \cdot 10^4$	$1.5 \cdot 10^7$